



# Pea protein isolate-based active films for salmon preservation: The role of different essential oils in film properties, antioxidant, and antibacterial activities

Jingjing Cheng, Nethraja Kandula, Victoria Eugenia Cortes, Hyuk Choi, Prashant Singh, Leqi Cui\*

Department of Health, Nutrition, and Food Sciences, Florida State University, Tallahassee, FL, 32306, USA

## ARTICLE INFO

Handling Editor: Dr. Quancai Sun

### Keywords:

Pea protein  
Essential oil  
Active packaging  
Antioxidant  
Antibacterial activity

## ABSTRACT

To improve the packaging properties of pea protein isolate (PPI) films, 2 wt% of essential oil (EO) from garlic, ginger, or cinnamon was individually incorporated into the films. The film properties were evaluated after the addition of EOs. The resulting PPI active films were applied to salmon to explore their efficacy in a real food system. The results indicated that the moisture content (MC), total soluble matter (TSM), water vapor permeability (WVP), water contact angle (WCA), tensile strength (TS), and elongation at break (EAB) of PPI film decreased after adding EOs, with the extent of the decrease varying based on the type of oil. SEM images revealed that the distribution of EOs within the film matrix differed: garlic EO was mainly distributed within the internal structure, while ginger and cinnamon EOs were primarily on the surface. FTIR analysis confirmed the interactions between PPI and EOs. When applied to salmon, garlic EO and ginger EO promoted lipid oxidation, whereas cinnamon EO significantly delayed it. Although PPI-based active films containing garlic or cinnamon EOs showed remarkable antibacterial activity in vitro, they did not inhibit bacterial growth in salmon. Additionally, EOs in active films may notably alter the color and sensory properties of salmon, potentially influencing consumer acceptance. Our findings demonstrated that the EO type is a key factor in influencing the properties of edible films. More importantly, the effectiveness of active films is closely related to the specific food system in which they are applied.

## 1. Introduction

Salmon is among the most favored fish by consumers worldwide. According to a report by [Grand View Research \(2022\)](#), the global market size for salmon was valued at \$14.87 billion in 2021, with an expected annual growth rate of 8.5% from 2022 to 2030. The popularity of salmon can be attributed to its rich nutrients and tender texture. However, its high content of protein, polyunsaturated fatty acids, and moisture makes salmon highly susceptible to spoilage, primarily due to microbial growth and lipid oxidation ([Yu et al., 2020](#)). This susceptibility leads to significant waste during transportation from production to consumers. To mitigate spoilage, traditional methods such as freezing, drying, canning, and fermentation are employed to extend the shelf life of salmon ([Kontominas et al., 2021](#)). However, these traditional methods are associated with certain limitations, including significant energy consumption, potential alterations in taste, and intricate

procedural requirements. In response to these challenges, researchers have recently attempted to develop edible active packaging films and coatings with antioxidant and antibacterial activities. These innovative packaging materials aim to improve the storage environment of salmon, thereby extending its shelf life ([Tan et al., 2024](#); [Vidal et al., 2024](#); [Zomorodian et al., 2023](#)).

Edible food packaging films are thin layers made from materials such as polysaccharides, proteins, and lipids, designed to wrap or coat food products ([Azeredo et al., 2022](#)). Traditional food packaging methods, typically reliant on synthetic plastics, pose significant environmental concerns due to their non-biodegradability and the accumulation of plastic waste. In contrast, edible packaging materials are designed to be consumed along with the food product or to biodegrade harmlessly, thus reducing the environmental footprint. Moreover, they can include antimicrobials and antioxidants, which are integrated into the packaging matrix to interact with the food product and its environment, thereby

\* Corresponding author.

E-mail address: [lcui2@fsu.edu](mailto:lcui2@fsu.edu) (L. Cui).

<https://doi.org/10.1016/j.crfs.2024.100936>

Received 16 August 2024; Received in revised form 22 November 2024; Accepted 24 November 2024

Available online 28 November 2024

2665-9271/© 2024 The Authors. Published by Elsevier B.V. This is an open access article under the CC BY-NC license (<http://creativecommons.org/licenses/by-nc/4.0/>).

inhibiting microbial growth, delaying oxidation, and maintaining food quality (Ghamari et al., 2022; Pérez Córdoba and Sobral, 2017). This particularly benefits fish products like salmon, which are prone to spoilage due to microbial growth and lipid oxidation.

Among the various raw materials of edible packaging, pea protein has gained increasing attention (Farshi et al., 2024). As the second most important plant protein in the food industry, pea protein offers a balanced amino acid profile, high nutritional value, low allergenicity, and is non-GMO (Ge et al., 2020). According to the International Grains Council (IGC), the global production of dry peas is projected to rise to 13.9 million tons in the market year 2023–2024, with Russia, Europe, and the United States as major contributors (Commodity Board, 2024). The high availability of pea protein enhances its application in the field of edible films. Furthermore, the packaging properties of pea protein films have been improved recently by various physical and chemical technologies (Cheng et al., 2023; Gao et al., 2023a; Santhosh et al., 2024). Nevertheless, the utilization of pea protein for the development of active packaging materials has not yet been thoroughly investigated.

With the increase in consumer demand for freshness and food safety, the interest and investment in active film are growing (Gao et al., 2024a). These films are designed to actively interact with the food products they cover, often incorporating various substances such as antimicrobials and antioxidants. Essential oils (EOs), extracted from plants through distillation or pressing, are naturally volatile aromatic substances known for their strong antioxidant and antimicrobial properties (Gao et al., 2024b). Incorporating EOs into packaging materials enables the gradual release of active components, inhibiting microbial growth, retarding the oxidation phenomenon, and reducing food spoilage (Rehman et al., 2020). However, the hydrophobic nature of EOs can interfere with the chain-to-chain polymer interactions in aqueous film-forming solutions, affecting the resultant film properties (Akhter et al., 2019). Additionally, studies have shown that different EOs have distinct effects on the tensile strength, elongation at break, and water vapor barrier properties of edible films (Saricaoglu and Turhan, 2020; Venkatachalam et al., 2023). Therefore, selecting the appropriate EOs, considering their chemical composition and polarity relative to the polymer matrix, is crucial for optimizing the performance of bioactive packaging materials, ensuring they effectively enhance food preservation while maintaining desirable mechanical and barrier properties.

This study focuses on garlic, ginger, and cinnamon EOs due to their strong antimicrobial and antioxidant activities (Liu et al., 2022; Noori et al., 2018; Wang et al., 2021). Additionally, These EOs are derived from common culinary spices, and were chosen with the consideration that they might harmonize with food flavors. Specifically, this study aims to develop pea protein isolates (PPI)-based active films by incorporating these EOs and to investigate their effects on the packaging properties of PPI films. The resulting films were evaluated for their mechanical properties, water barrier properties, optical properties, microstructure, and in vitro antibacterial activities. Fourier-transform infrared spectroscopy (FTIR) was used to determine the interactions between the EOs and PPI. Finally, active films were applied to salmon packaging to assess their effectiveness in extending the shelf life of salmon through their antimicrobial and antioxidant activities, and their influence on salmon flavor.

## 2. Materials and methods

### 2.1. Materials

Yellow pea protein isolate (PPI) was procured from Naked Nutrition (Miami, FL, USA) with protein, fat, and carbohydrate contents of 90%, 2%, and 7%, respectively. Pure garlic essential oil (*Allium sativum*; origin from China; steam distilled bulb), ginger essential oil (*Zingiber officinale*; origin from India; steam distilled root), and cinnamon essential oil (*Cinnamomum zeylanicum*; origin from Ceylon; steam distilled leaf) were obtained from Silky Scents, LLC. (Corona, CA, USA).

Glycerol ( $\geq 99\%$ ) was sourced from Sigma (St. Louis, MO, USA). Bacterial strains, including *Salmonella* Typhimurium (ATCC 14028), *Escherichia coli* 045–1, and *Staphylococcus aureus* (NCTC 8532) were acquired from the Food Microbiology Laboratory Culture Collection of Florida State University (Tallahassee, FL, USA). All other solvents and reagents utilized were of analytical grade or higher purity.

### 2.2. Preparation and characterization of EO emulsions

The method prepared the EO emulsions were referred to a previous study with some modifications (Liao et al., 2021). PPI was used as an emulsifier to prepare essential oil-in-water emulsions. Specifically, PPI (2%, w/w), EO (10%, w/w), and deionized water were mixed using a high-speed homogenizer (IKA T25 digital ultra-turrax, Staufen, Germany) at 13,000 rpm for 3 min. The coarse emulsions were subjected to high-pressure processing at 20,000 psi with 2 passes at 2 L/h flow rate using a high-pressure homogenizer (Nano DeBEE, BEE International, USA). A heat exchanger utilizing cold water flow was utilized to prevent temperature elevation during homogenization. Freshly prepared emulsions were used for subsequent film-forming solution preparation. The average droplet size ( $z$ -average), poly-dispersity index (PDI), and zeta potential of the emulsions were determined using a Zeta-sizer (Nano ZS90, Malvern Instruments, UK), following the method outlined by Cui et al. (2019) with minor adaptations. Before measurement, emulsions were diluted 125-fold to mitigate the effects of multiple scattering, and all measurements were performed at 25 °C. The refractive indices used for particle and dispersant phase are 1.59 and 1.33, respectively.

### 2.3. Development and evaluation of essential oil-loaded PPI films

#### 2.3.1. Film production

The preparation of PPI-based films followed the method described in our previous study (Cheng et al., 2024). Briefly, PPI was dissolved in deionized water and stirred for 4 h. Then, EO emulsions were added to the dispersion to reach a final EO content of 2% (w/w) and a total PPI concentration of 7.5%. Glycerol (50% w/w of protein) was added as a plasticizer to the film-forming dispersions and stirred for 30 min. After degassing, 15 mL of the prepared dispersions were poured onto Petri dishes with a diameter of 10 cm and dried for 24 h at 25 °C. Control film without EO was also prepared using PPI alone. Higher concentrations of EO were not explored due to concerns about disrupting the film structure. Once dried, the films were peeled off and conditioned for 3 day at 55% relative humidity and 25 °C.

#### 2.3.2. Film thickness, moisture content (MC), and total soluble matter (TSM)

Film thickness was assessed utilizing a manual digital micrometer with an accuracy of 0.01 mm, measuring at five random points across each film. The MC and TSM were measured according to the method described in a previous study (Muñoz et al., 2012). The film was initially sectioned, each piece weighed meticulously, and then subjected to 105 °C in an oven for 24 h. Following this, the samples were re-weighed, and the moisture content (MC) was determined based on the weight loss percentage. For total soluble matter (TSM) measurement, the dried film pieces were immersed in 30 mL of deionized water at 25 °C for 24 h. Subsequently, the undissolved film pieces were filtered using pre-weighed, desiccated filter paper, dried at 105 °C for 24 h, and weighed to ascertain the weight of insoluble dry matter. TSM was the percentage of the soluble dry matter weight relative to the initial dry matter weight.

#### 2.3.3. Water vapor permeability (WVP)

Following the ASTM Standard Test Method (ASTM, 1995), the water vapor permeability (WVP) was assessed. Each film, measuring 2 cm × 2 cm, was sealed atop a glass vial pre-filled with silica gel. These vials were placed in a chamber conditioned with deionized water and

weighed every 12 h over 2 days. WVP was determined using the following calculation:

$$WVP = \frac{\Delta m \times l \times \Delta p}{\Delta t \times A}$$

Where:

$\Delta m/\Delta t$  is the rate of weight gain over time;  $A$  represents the area of the film exposed to the environment ( $m^2$ );  $l$  denotes the thickness of the films (mm);  $\Delta p$  signifies the partial vapor pressure difference across the two sides of the film (2.895 kPa).

#### 2.3.4. Tensile strength (TS) and elongation at break (EAB)

The measurement of TS and EAB was adopted from a previous study with some modifications (Venkatachalam et al., 2023). Specifically, film strips measuring 60 mm in length and 20 mm in width were prepared. The film strip was stretched using a texture analyzer (Stable Micro System Ltd., Godalming, UK) to test its TS and EAB. During this process, the strip was vertically secured onto the texture analyzer by two grips initially spaced 20 mm apart. TS was determined by dividing the maximum load by the cross-sectional area of the film strip (20 mm  $\times$  film thickness). EAB was defined as the ratio between the maximum elongation distance (mm) and the initial distance (20 mm).

#### 2.3.5. Water contact angle (WCA)

WCA values were determined by placing a 3  $\mu$ L droplet of deionized water onto the film surface at 25 °C using a drop shape analyzer (DSA25, Kruss, Germany). The analyzer captured the image of the droplet, and the WCA was calculated using KRÜSS ADVANCE software (Kruss, Germany).

#### 2.3.6. Color and opacity

Film color was assessed using a colorimeter (LabScan XE, HunterLab, Reston, VA, USA), with results presented as  $L$  (darkness/whiteness),  $a$  (greenness/redness), and  $b$  (blueness/yellowness) values. Measurements were taken from five different spots on each film to ensure accuracy and representativeness. The opacity of film was measured by calculating the ratio of its absorbance at 600 nm to its thickness in millimeters.

#### 2.3.7. Scanning electron microscopy (SEM)

A field emission scanning electron microscope (JSM-IT800, JEOL Ltd., Japan) was employed to examine the microstructure and morphology of the films. The SEM test was referred to a previous study with some modifications (Fathi et al., 2018). To prepare the samples, films were fractured manually using liquid nitrogen to create suitable cross-sections for analysis. These fractured sections were then mounted on a holder and coated with uranium using a Cressington Carbon Coater (Cressington Scientific Instruments Ltd., Watford, UK). The microscope operated at an accelerating voltage of 5.0 kV for imaging. The SEM detector is Secondary Electron Detector (SED) and the working distance was in the range of 10–12 mm. Surface images were taken at magnifications of 300  $\times$  and 3000  $\times$ , whereas cross-sectional images were taken at magnifications of 300  $\times$  and 1500  $\times$ .

#### 2.3.8. Fourier transform infrared spectroscopy (FTIR)

The structural properties of films were examined using an FTIR spectrometer system coupled with an attenuated total reflectance attachment (FTIR-ATR) (JASCO 6800, JASCO, Japan), following the method described in a previous study (Cheng et al., 2022). The spectra range was 4000 to 400  $cm^{-1}$ , and the resolution was 4  $cm^{-1}$  over 64 scans. Background data were collected before scanning. After the measurement, the spectra underwent processing, including noise elimination, baseline correction, and Savitzky-Golay smoothing (25 convolution points), to ensure precise analysis.

## 2.4. In vitro antibacterial activity

Foodborne pathogens significantly contribute to food spoilage and reduce shelf life. The antibacterial activity of PPI-based films, incorporating various essential oils, was evaluated using the disk diffusion assay against three bacterial strains: *Salmonella* Typhimurium, *E. coli*, and *S. aureus*. The method was referred from a prior study with some modifications (Hematizad et al., 2021). In brief, an isolated colony was selected and diluted using 0.85% saline until reaching turbidity of 0.5 McFarland units, yielding an inoculum with approximately  $1.5 \times 10^8$  CFU/mL of bacteria. A 100  $\mu$ L sample was evenly spread on Mueller-Hinton agar plates. Meanwhile, films were cut to a diameter of 15 mm, sterilized with UV light, and placed on the inoculated media. After incubation at 35 °C for 24 h, the antibacterial activity was evaluated by measuring the inhibition zones around the film discs. These measurements were recorded in millimeters (mm). Duplicate measurements were performed for each film.

## 2.5. Preparation of salmon samples

The experimental procedure involved sourcing fresh skinless salmon fillets from a local market. On Day 0, the day the salmon arrived, measurements of peroxide value, TBARS, aerobic plate count, and pH were taken from the fresh samples, all of which were sourced from the same batch. These fillets were then sliced into chunks, each weighing around 50 g. Subsequently, the salmon samples were coated with different film-forming dispersions. Each sample was submerged in 600 mL of the respective dispersion for 30 s, followed by a draining period of 20 min. The control group received a treatment of cold deionized water to simulate potential bacterial removal and moisture uptake. After coating, the individual salmon samples were placed on trays, wrapped with cling film, and stored at 4 °C for a period of 9 days to facilitate subsequent quality evaluation.

## 2.6. Evaluation of lipid oxidation

### 2.6.1. Peroxide value

The method was referenced to previous studies with slight modifications (Cui et al., 2018; Yarnpakdee et al., 2012). 1 g of ground sample was added in 14 g of chloroform/methanol (2:1, v/v) solution and vortexed for 2 min. The mixture was then centrifuged at 4000 rpm for 5 min. Afterward, 7 mL of the lower phase was mixed with 2 mL of 0.5% NaCl. The mixture was then vortexed for 30 s and centrifuged at 4000 rpm for 5 min to separate into two phases. 1.5 mL of the bottom phase was mixed with 7.5  $\mu$ L of 0.072 M ferrous sulfate and 7.5  $\mu$ L of 3.94 M ammonium thiocyanate and vortexed. The reaction mixture was allowed to stand for 20 min and then centrifuged at 10,000 rpm for 5 min. The absorbance of the supernatant was measured at 500 nm. The blank was prepared similarly, except that 1.5 mL of chloroform/methanol (2:1, v/v) was used instead of the sample. A standard curve was constructed using cumene hydroperoxide over a 2.5–30  $\mu$ M concentration range.

### 2.6.2. Measurement of thiobarbituric acid reactive substances (TBARS)

Thiobarbituric acid-reactive substances (TBARS) were determined as described by (Lee et al., 2024) with some modifications. The ground sample (1.0 g) was homogenized with 5 mL of TBA, a solution containing 0.375% thiobarbituric acid (w/v), 15% trichloroacetic acid (w/v), and 0.25 M HCl. The mixture was heated in a boiling water bath (95–100 °C) for 20 min to develop a pink color. After heating, it was cooled to room temperature using tap water and then centrifuged at 4000 rpm for 5 min. The absorbance of the supernatant was measured at 532 nm. For the blank, 1 mL of deionized water was used instead of the sample. A standard curve was generated using 1,1,3,3-tetramethoxypropane at concentrations ranging from 5 to 40  $\mu$ M. The TBARS value was calculated and expressed as mg of malonaldehyde per kg of sample.

**Table 1**

The particle size (z-average), particle (PDI), and zeta-potential of garlic, ginger, and cinnamon essential oil-in-water emulsions.

Emulsion	Z-average (nm)	PDI	Zeta-potential (mV)
Garlic	327.33 ± 6.71 <sup>b</sup>	0.25 ± 0.03 <sup>a</sup>	-22.87 ± 0.76 <sup>a</sup>
Ginger	425.60 ± 12.08 <sup>c</sup>	0.39 ± 0.03 <sup>b</sup>	-26.80 ± 0.82 <sup>b</sup>
Cinnamon	269.30 ± 9.00 <sup>a</sup>	0.22 ± 0.00 <sup>a</sup>	-36.67 ± 0.64 <sup>c</sup>

Different letters within the same column are significantly different ( $p < 0.05$ ).

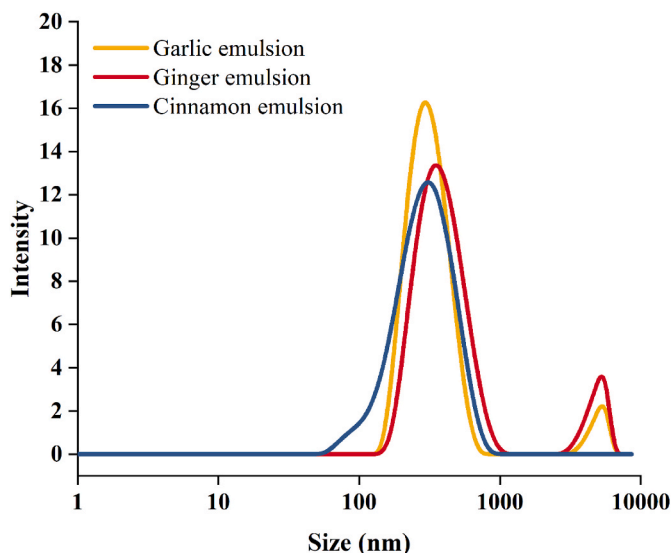


Fig. 1. Particle size distribution of garlic, ginger, and cinnamon essential oil-in-water emulsions.

### 2.7. Microbiological analysis

Serial dilutions were conducted with salmon samples (25 g) and 0.1% peptone water (225 mL). Mesophilic microorganism assessment was performed using Plate Count Agar (PCA; BD Difco, Le Pont de Claix, France) and incubated at 35 °C for 24 h and 25 °C for another 24 h. Microbiological analyses were performed in duplicate at each storage interval, and the microbial counts obtained were converted to log values of colony-forming units per gram (log CFU/g).

### 2.8. Determination of pH

The pH of the salmon was determined according to the method in a previous study (Fu et al., 2024). 5 g of salmon samples were mixed with 50 mL of deionized water and shaken for 10 min at 280 rpm. The mixture was then filtered, and the pH of the supernatant was measured.

### 2.9. Sensory evaluation

The fresh samples were cooked in an oven at 200 °C for 20 min. Sensory evaluation was conducted following a previously established protocol (Vital et al., 2018). Ten semi-trained panelists participated in the evaluation of sensory attributes, including color, odor, taste, tenderness, and overall acceptability. A 9-point hedonic scale was utilized to evaluate consumer acceptance, with scores defined as follows: 9 - Like extremely, 8 - like Very Much, 7 - Like Moderately, 6 - Like Slightly, 5 - Neither Like nor Dislike, 4 - Dislike Slightly, 3 - Dislike Moderately, 2 - Dislike Very Much, and 1 - Dislike Extremely. Cooked samples were presented to the panelists in a randomized design to minimize potential carry-over effects. The evaluation was performed under controlled conditions to ensure consistency across all assessments.

### 2.10. Statistical analysis

Experiments were carried out in triplicate unless otherwise specified, and results are presented as the mean ± standard deviation (SD). Statistical significance was assessed using Duncan's multiple comparison test, with a threshold of  $p < 0.05$ , utilizing SPSS version 25.0 (SPSS Inc., Chicago, IL, USA).

## 3. Results and discussion

### 3.1. Droplet size, PDI, and zeta potential of EO emulsions

The average droplet sizes (z-average), particle size distribution indices (PDI), and zeta potentials of oil-in-water emulsions prepared using different EOs are shown in Table 1. Significant differences in average droplet size were observed among emulsions of different EOs. The ginger oil emulsion exhibited the largest average droplet size at 425.60 nm, followed by the garlic oil emulsion at 327.33 nm, and the cinnamon oil emulsion with the smallest droplet size at 269.30 nm. Correspondingly, the PDI values also varied. The ginger oil emulsion has the highest PDI value at 0.39, followed by the garlic oil emulsion at 0.25 and the cinnamon oil emulsion at 0.22. These findings are further corroborated by the droplet size distributions shown in Fig. 1, where both the garlic and ginger oil emulsions displayed bimodal distributions. In contrast, the cinnamon emulsion exhibited a unimodal distribution with a left shift, indicating a higher portion of smaller droplets. The above results indicate that when preparing oil-in-water emulsions, the characteristics of the emulsion vary depending on the type of oils used, even when the same emulsifier is applied. Similarly, Gomes et al. (2018) observed that the droplet size of LCT emulsions was larger than that of MCT emulsions when WPI/Tween 80 was used as the emulsifier. They attributed the variances to the different viscosity of oils; lower viscosity allows the oil droplets to break up into smaller sizes. Additionally, it is known that emulsion formation is influenced by the interfacial tension between the oil and water phases (McClements, 2015). Reduced interfacial tension can facilitate emulsion formation by reducing the free energy required to deform and disrupt the droplets. In this study, the different chemical compositions, oil polarities, molecular weights, and chain lengths of various EOs may alter the interfacial tension, thus affecting the emulsion properties. Understanding the characteristics of EO emulsions is essential as the distribution of oil droplets within the film matrix significantly impacts interactions among the polymers forming the film, the oil molecules, and the water molecules. These interactions, in turn, alter film properties (Acevedo-Fani et al., 2015). The discrepancies observed among different essential oil emulsions emphasize the critical importance of selecting appropriate EOs to achieve optimal film packaging properties.

The electrical charge of oil droplets is important to stabilize emulsions through electrostatic repulsion. Differences in electrostatic repulsion among oil droplets may affect the intermolecular interactions (repulsion or attraction) among film-forming particles, thereby altering the film structure and influencing the film properties (Li et al., 2020). As shown in Table 1, the zeta potentials of the oil droplets in the three emulsions were distinct. Specifically, the emulsion prepared with cinnamon EO exhibited the highest absolute value of zeta potential, followed by the emulsion with ginger EO, and then the emulsion with garlic EO. Consistent with our results, Taha et al. (2018) observed significant differences in the zeta potential values of MCT, palm, soy, and rapeseed oil droplets in emulsions stabilized by SPI. They attributed these differences to the varying amounts of protein content at the oil/water interface, which is influenced by the differing water solubility of the oils. Moreover, the potential presence of ionized groups in EO compositions may also modify the surface charge distribution of oil droplets (Acevedo-Fani et al., 2015).



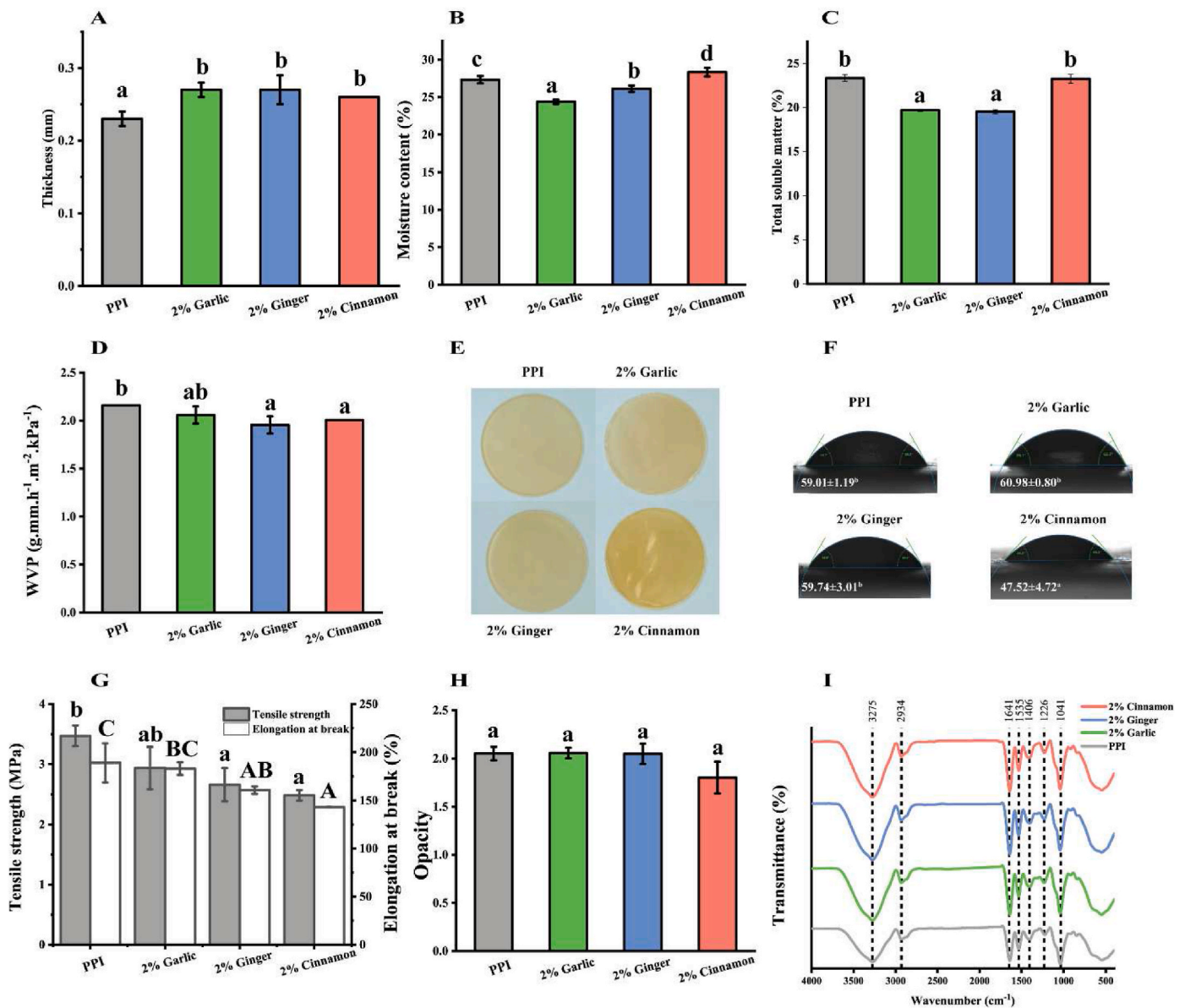


**Fig. 2.** The (A) thickness, (B) moisture content (MC), (C) total soluble matter (TSM), (D) water vapor permeability (WVP), (E) water contact angle (WCA), (F) tensile strength (TS) and elongation at break (EAB), (H) opacity, and (I) FTIR spectra of PPI-based active films loaded with garlic, ginger, or cinnamon essential oil.

### 3.2. Characterization of PPI-based films loaded with different essential oils

#### 3.2.1. Film thickness

As shown in Fig. 2A, the thickness of the PPI film was 0.23 mm. After adding EOs into the film matrix, the thickness increased by 13%–17%. The increase is not surprising since the addition of EOs affects the intermolecular forces within the film matrix, leading to changes in film density, which is one of the factors influencing film thickness (Zomorodian et al., 2023).

#### 3.2.2. Moisture content (MC) and total soluble matter (TSM)

The MC and TSM are critical indicators for assessing the water-resistant performance of edible films as packaging materials. Fig. 2B depicts the MC of PPI-based films loaded with different EOs. It was observed that incorporating different types of EOs into the film matrix had varied effects on the MC. Specifically, compared to the PPI film, the presence of garlic and ginger EOs significantly reduced the MC to 24.40% and 26.14%, respectively, whereas cinnamon EO slightly

increased the MC. Venkatachalam et al. (2023) also found that different EOs affected the MC differently when studying the influence of incorporating different essential oils on the physicochemical properties of chitosan composite edible films. They reported that garlic EO notably decreased MC, followed by turmeric oil, while galangal oil and kaffir lime had no significant effect.

Total soluble matter (TSM) is another indicator of the hydrophobicity or hydrophilicity of edible films. The results in Fig. 2C show a decrease in TSM after adding garlic or ginger EOs to PPI films, whereas cinnamon EO addition did not change the TSM. A similar reduction was observed when incorporating clove and cinnamon oils into chitosan films but not thyme essential oil (Hosseini et al., 2009). In addition, Teixeira et al. (2014) studied the characterization of fish protein films with EOs of clove, garlic, and oregano, finding that adding these EOs reduced film solubility, although the degree of reduction varied.

The MC and TSM of edible films based on proteins and polysaccharides are largely determined by the interactions between water molecules and polymers that stabilize the film structure. The addition of EOs to edible films may reduce the MC and TSM due to the interaction of

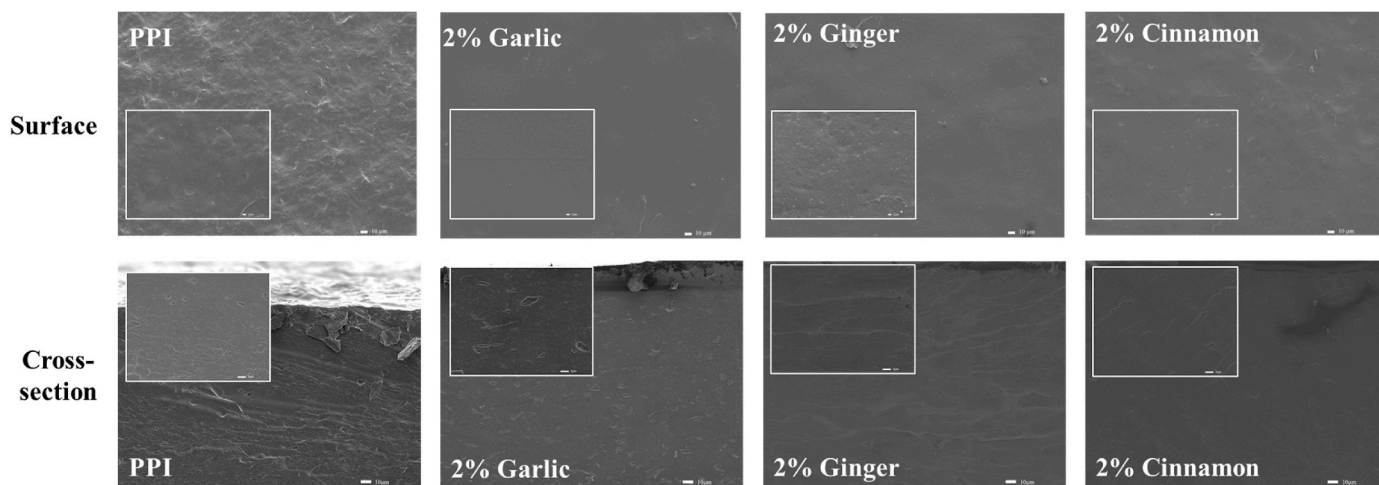


**Fig. 3.** The SEM micrographs of surfaces (at  $\times 300$  magnification and  $\times 3000$  magnification [inlet]) and cross-sections (at  $\times 300$  magnification and  $\times 1500$  magnification [inlet]) of PPI-based active films loaded with garlic, ginger, or cinnamon essential oil.

**Table 2**

The *L*, *a*, and *b* values of PPI-based active films loaded with garlic, ginger, or cinnamon essential oil.

Film	<i>L</i>	<i>a</i>	<i>b</i>
PPI	82.93 $\pm$ 0.23 <sup>c</sup>	-0.70 $\pm$ 0.03 <sup>a</sup>	24.92 $\pm$ 0.44 <sup>a</sup>
2% garlic	81.79 $\pm$ 0.24 <sup>b</sup>	-0.02 $\pm$ 0.13 <sup>b</sup>	28.55 $\pm$ 0.46 <sup>b</sup>
2% ginger	82.55 $\pm$ 0.27 <sup>c</sup>	-0.78 $\pm$ 0.14 <sup>a</sup>	28.91 $\pm$ 0.98 <sup>b</sup>
2% cinnamon	79.98 $\pm$ 0.25 <sup>a</sup>	1.03 $\pm$ 0.18 <sup>c</sup>	40.16 $\pm$ 0.86 <sup>c</sup>

Different letters within the same column are significantly different ( $p < 0.05$ ).

**Table 3**

In vitro antimicrobial activity of PPI-based active films loaded with garlic, ginger, or cinnamon essential oil.

Film	Inhibition zone (mm)		
	<i>S. Typhimurium</i>	<i>E. coli</i>	<i>S. aureus</i>
PPI	ND	ND	ND
2% garlic	ND	ND	57.50 $\pm$ 0.00
2% ginger	ND	ND	ND
2% cinnamon	19.50 $\pm$ 0.71	21.50 $\pm$ 0.71	21.50 $\pm$ 2.12

ND: Not detected.

film-forming polymers with the hydrophobic EOs, which decreases the affinity of the polymers for water molecules (Akhter et al., 2019). On the other hand, due to the variations in the polarities of different EOs, the interactions among polymers, EOs, and water molecules in the film matrix can vary. This could result in different degrees of MC and TSM reduction. In this study, we found that incorporating garlic and ginger EOs into PPI films reduced the MC and TSM, thereby enhancing the hydrophobicity of the films. In contrast, cinnamon EO had no significant effect on these properties.

### 3.2.3. Water vapor permeability (WVP)

The water vapor permeability (WVP) directly affects the ability of films to regulate moisture transfer between packaging and food. Incorporating different essential oils (EOs) into the PPI film matrix altered its WVP. As depicted in Fig. 2D, adding garlic EO did not significantly reduce WVP, whereas ginger and cinnamon EOs led to a notable decrease in WVP of PPI films. EOs are known to influence WVP by either increasing the tortuosity of water vapor pathways or inducing phase separation within the film matrix, thereby enhancing or impairing moisture barrier properties (Cai and Wang, 2021; Cheng et al., 2024; Haghghatpanah et al., 2022). Our findings highlight that ginger and

cinnamon EOs effectively reduce WVP in PPI films, improving their moisture resistance.

### 3.2.4. Water contact angle (WCA)

Water contact angle (WCA) is another important parameter to evaluate the hydrophobicity of packaging materials. The effect of adding different EOs to PPI films on WCA is shown in Fig. 2F. The WCA of PPI film is 59.01°, which is consistent with a previous study reporting WCA of PPI film is 56.48° (Gao et al., 2023b). The addition of garlic or ginger EOs did not significantly change the WCA of PPI films. However, it was found that cinnamon EO incorporation led to a significant decrease in the WCA of PPI film. Contrary to our findings, Bahram et al. (2014) reported that cinnamon EO could significantly increase the WCA of whey protein films. Previous studies have attributed the decrease in film surface wettability with EO incorporation to the hydrophobic nature of EO (Hasheminya and Dehghannya, 2021; Yu et al., 2022). However, the impact of lipids, including EOs, on the WCA of the edible film surface may be influenced by other factors. These factors include the interruption of hydrophobic interactions between the continuous phase by oil droplets, leading to the projection of hydrophilic or polar groups of protein molecules to the surface, thereby increasing surface wettability. Additionally, the roughness of the film surface, a key factor determining surface wettability, may be altered by the presence of lipids (Cheng et al., 2024). The varying effects of different EOs on the WCA of PPI films could result from the interaction of multiple factors.

### 3.2.5. Mechanical properties

Tensile strength (TS) and elongation at break (EAB) were tested to evaluate the mechanical properties of PPI-based films containing different EOs. As shown in Fig. 2G, the addition of garlic EO did not significantly change the TS and EAB of PPI film, but ginger and cinnamon EOs resulted in a significant decrease in both TS and EAB. Many studies have demonstrated that incorporating EOs can reduce the mechanical properties of edible films by disrupting film structure and reducing the cohesive force within the structure (Li et al., 2020; Zúñiga et al., 2012). In this study, The microstructure changes of PPI films support the standpoint. As shown in Fig. 3, the presence of oil droplets on the film surface and in the internal film matrix (cross-sectional images) interrupted the hydrocolloid matrix and increased the heterogeneity of the film. Additionally, we observed that the extent of reduction in TS and EAB of PPI films was dependent on the type of EO used. Cinnamon EO caused the greatest reduction, while garlic EO resulted in the least reduction. Similarly, Venkatachalam et al. (2023) reported that different EOs incorporation could have distinct impacts on the

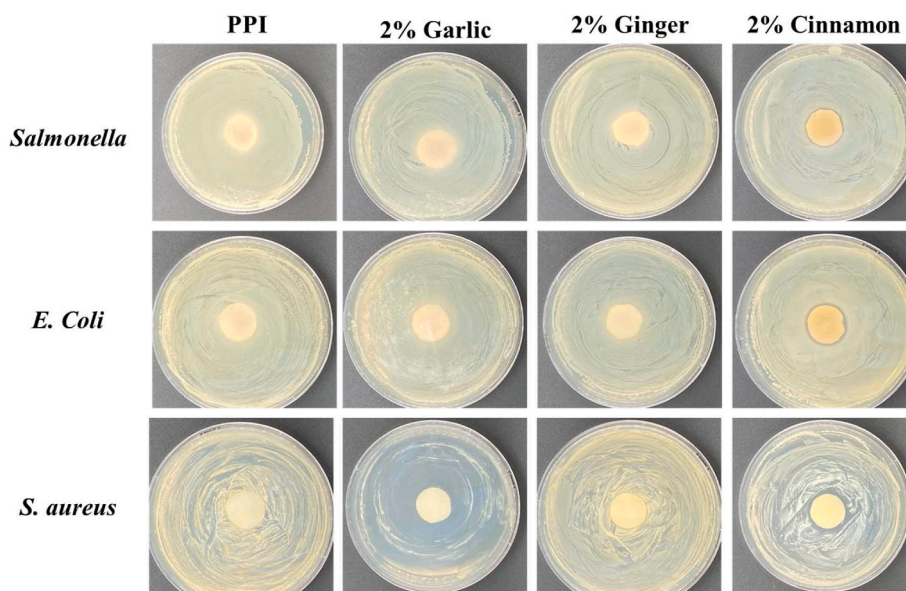


Fig. 4. The inhibition zones of PPI-based active films against *Salmonella*, *E. coli*, and *Staphylococcus aureus*.

mechanical properties of chitosan and rice starch-based films. This could be explained by the variations in the electrical charge of oil droplets in the film structure (zeta potential as shown in Table 1). The repulsive forces among polymers with the same charge could influence the distance between polymers, thus affecting flexibility (Acevedo-Fani et al., 2015).

### 3.2.6. Color and opacity

The color of PPI films is reflected by  $L$ ,  $a$ , and  $b$  values. As we can see in Table 2, the  $L$  values decreased when either garlic EO or cinnamon EO was added to the films, while the  $a$  values increased. This indicates that the presence of garlic or cinnamon EOs caused the PPI films to become darker and reddish. However, the addition of ginger EO did not change  $L$  or  $a$  value significantly. Regarding the  $b$  value, three EOs significantly increased the  $b$  value of the films, with cinnamon EO causing the greatest increase in yellowness. Other studies also found that the incorporation of EOs into the film matrix can significantly change the color of the films, and the color change is associated with the oil type (Kowalczyk et al., 2016; Venkatachalam et al., 2023). The significant differences in the effects of different types of EOs on the color of edible films may be due to the particle size of the dispersed phase, the heterogeneity of film structures, and the differences in refractive indexes between phases in composite films, which can influence light scattering and thus affect the optical properties of films (Fabra et al., 2009).

However, no differences in opacity were observed among the PPI films, as illustrated in Fig. 2H. This may be attributed to the inherently good opacity of PPI films, with the addition of a small amount of EOs being insufficient to alter their original light transmission properties. Similarly, Kowalczyk et al. (2016) found that the incorporation of oleic acid, regardless of the concentration, did not affect the opacity of PPI films. They explained that the incorporation of liquid lipids is less effective in increasing film opacity than solid lipids.

### 3.2.7. SEM

The microstructures of PPI films incorporating various EOs are displayed in Fig. 3, including surface and cross-sectional images. As we can see, The surface of the PPI film was rough, with granular protrusions. Although some pores were present on the surface of the film, the overall structure was dense. Observing the cross-section, the film texture was layered and stacked, with pores and cracks distributed throughout. This observation aligns with the microstructure of PPI films as reported in a previous study (Kowalczyk et al., 2016). Both studies demonstrate that

PPI particles are tightly packed and interconnected within the film matrix due to cohesive forces. The addition of EOs into PPI films significantly altered the film structure. Upon EO addition, the granules on the film surface vanished, rendering it noticeably smoother, while the internal structure became more flattened. This shift occurred as the forces maintaining the film structure transitioned from protein-protein interactions to a combination of protein-protein, protein-oil, and oil-oil interactions. Additionally, the presence of EOs notably increased the formation of pores and cracks on both the film surface and within its internal structure, rendering the structure more heterogeneous. This structural transformation elucidates the reduction in the mechanical properties of PPI films containing EOs. Several studies have also documented the presence of pores in film matrices following the addition of EOs (Cai et al., 2020; Cai and Wang, 2021; Moghimi et al., 2017). These pores could be the aggregation of oil droplets. Notably, the distribution of pores in the films varied. In the PPI-based films containing garlic EO, the pores were mainly located within the internal structure (cross-section), whereas in the PPI-based films loaded with ginger or cinnamon EOs, the pores were primarily found on the surface. Acosta et al. (2016), in their study on the effects of incorporating different EOs into starch-gelatin films, also noted distinct footprints of cinnamon, clove, and oregano EOs in the film matrix. These variations may stem from differences in the polarity, charge, and volatility of the EOs, influencing the flocculation, coalescence, and creaming effects of oil droplets during the film drying process, thus altering the film structure differently.

### 3.2.8. FTIR

FTIR spectroscopy (Fig. 2I) was used to identify the potential formation of chemical modification due to the presence of EOs. The spectra of PPI-based films with varying formulations displayed both similarities and differences. Specifically, seven peaks were identified in the FTIR spectra of PPI-based films:  $1641\text{ cm}^{-1}$  for Amide I,  $1535\text{ cm}^{-1}$  for Amide II, and  $1226\text{ cm}^{-1}$  for Amide III, which are characteristic of the protein backbone (Kumari et al., 2021). Additionally, peaks at  $3275\text{ cm}^{-1}$  (free -OH stretching vibration),  $2934\text{ cm}^{-1}$  (-CH stretching vibration),  $1406\text{ cm}^{-1}$  (carboxylate symmetric stretching vibration), and  $1041\text{ cm}^{-1}$  were observed. However, the intensities of the peaks varied for PPI-based films incorporating EOs compared to pure PPI films. Especially, the intensities of  $3275\text{ cm}^{-1}$  significantly increased for PPI-based films containing EOs, indicating the hydrogen bonds formed by water and PPI were altered by the disruption of EOs, thereby changing the absorbance of -OH. Similar results were observed in other studies



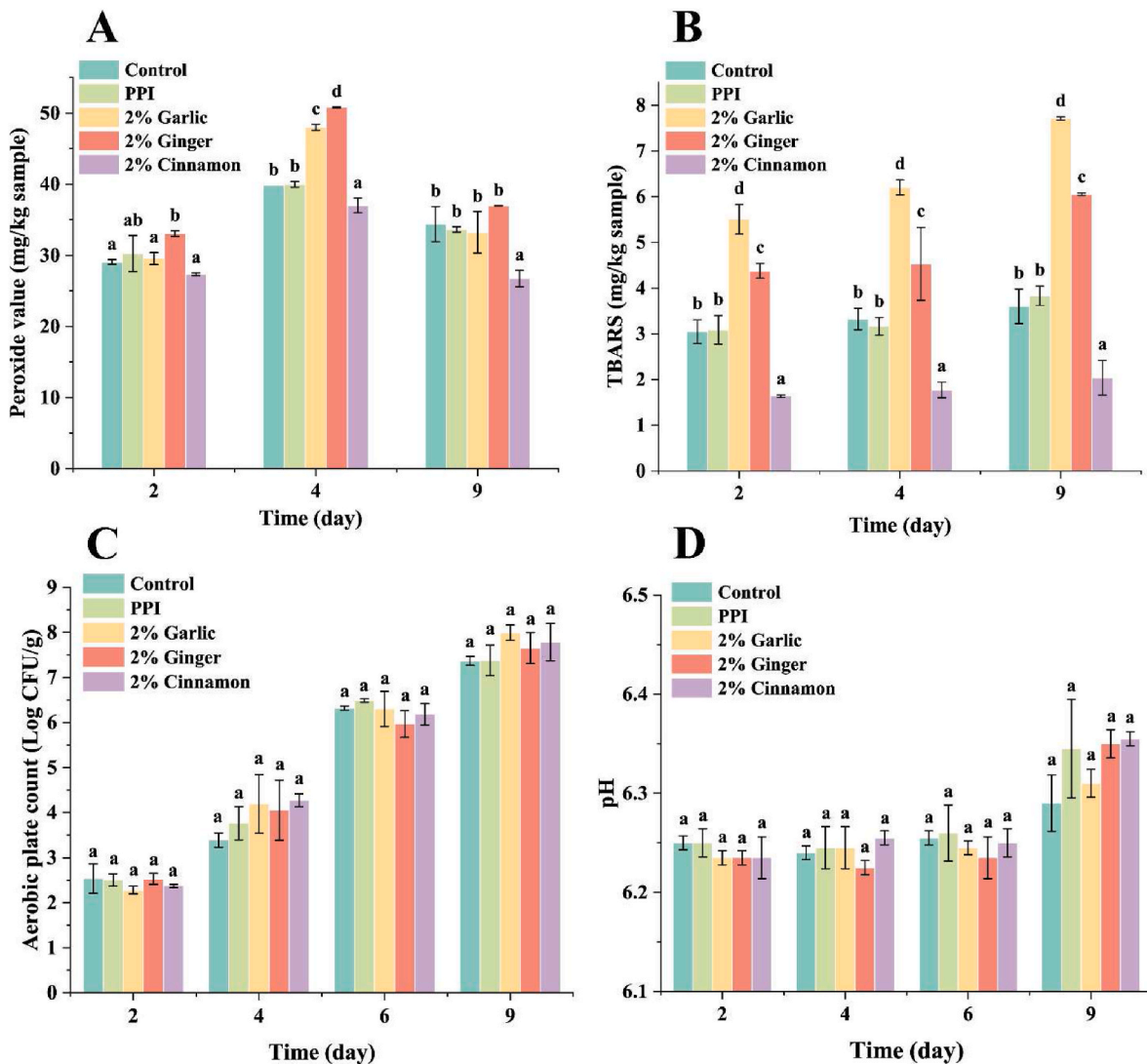


Fig. 5. The (A) peroxide value (PV), (B) TBARS, (C) aerobic plate count (APC), and (D) pH values of salmon treated with PPI-based active films loaded with garlic, ginger, or cinnamon essential oil at 4 °C over 9 days. Different letters indicate a significant difference between groups at the same storage time.

(Al-Harrasi et al., 2022; Xu et al., 2019). Furthermore, the intensity of the three characteristic peaks of pea protein significantly increased in films with the existence of EOs. Again, it suggests that interactions between PPI and essential oils occurred, disrupting the original interactions of protein particles.

### 3.3. Application of PPI-based active films on salmon

#### 3.3.1. Evaluation of lipid oxidation

Lipid oxidation is one of the important factors that determine food spoilage. To evaluate the effect of different EOs on the lipid oxidation of salmon, the peroxide value (PV) and the TBARS value were measured. On Day 0, the initial PV was 23.69 mg/kg sample, and the TBARS value was 1.37 mg/kg sample. Fig. 5A shows that the PV of the control sample gradually increased during the first four days of storage and then decreased by Day 9, indicating that lipid oxidation may have entered a later stage. Meanwhile, the TBARS values (Fig. 5B) exhibited a consistent upward trend. Significant differences in the extent of lipid oxidation were observed among the samples. Compared to the control, there were no significant differences in PV and TBARS values for samples treated with PPI, indicating that PPI alone did not exhibit antioxidant activity in salmon. However, samples treated with PPI loaded with 2% garlic or 2% ginger EO showed significantly higher PV and TBARS values than the

control, suggesting that both EOs accelerated lipid oxidation in salmon. In contrast, the group treated with the PPI-based film containing 2% cinnamon EO exhibited significantly lower PV and TBARS values compared to the other groups. Since the production of TBARS is a major source of off-flavors in spoiled food, the significant inhibitory effect of cinnamon EO indicates its ability to effectively prevent lipid oxidation and off-flavors in salmon, thereby preserving its quality.

Although EOs are generally believed to have antioxidant activity, some EOs exhibit pro-oxidant effects when applied to food (Aşık and Candoğan, 2014; Wang et al., 2018). This variation is due to the complex interactions within the food system. Firstly, the compositions of different EOs greatly influence their antioxidant activities. Phenolic compounds, the main active components of EOs, effectively scavenge peroxy radicals during lipid oxidation, thereby delaying the process. However, non-phenolic terpenoids can react with peroxy radicals to form reactive alkyl radicals, increasing the overall number of radicals in the system (Amorati et al., 2013). Consequently, the effective antioxidant activity of EOs results from a combination of both antioxidant and pro-oxidant actions. Additionally, the antioxidant/pro-oxidant effects of EOs are concentration-dependent (Pateiro et al., 2018). For example, while 150 ppm of rosemary essential oil can inhibit lipid and protein oxidation, higher concentrations (300 and 600 ppm) may promote oxidation reactions depending on the types of fatty acids involved



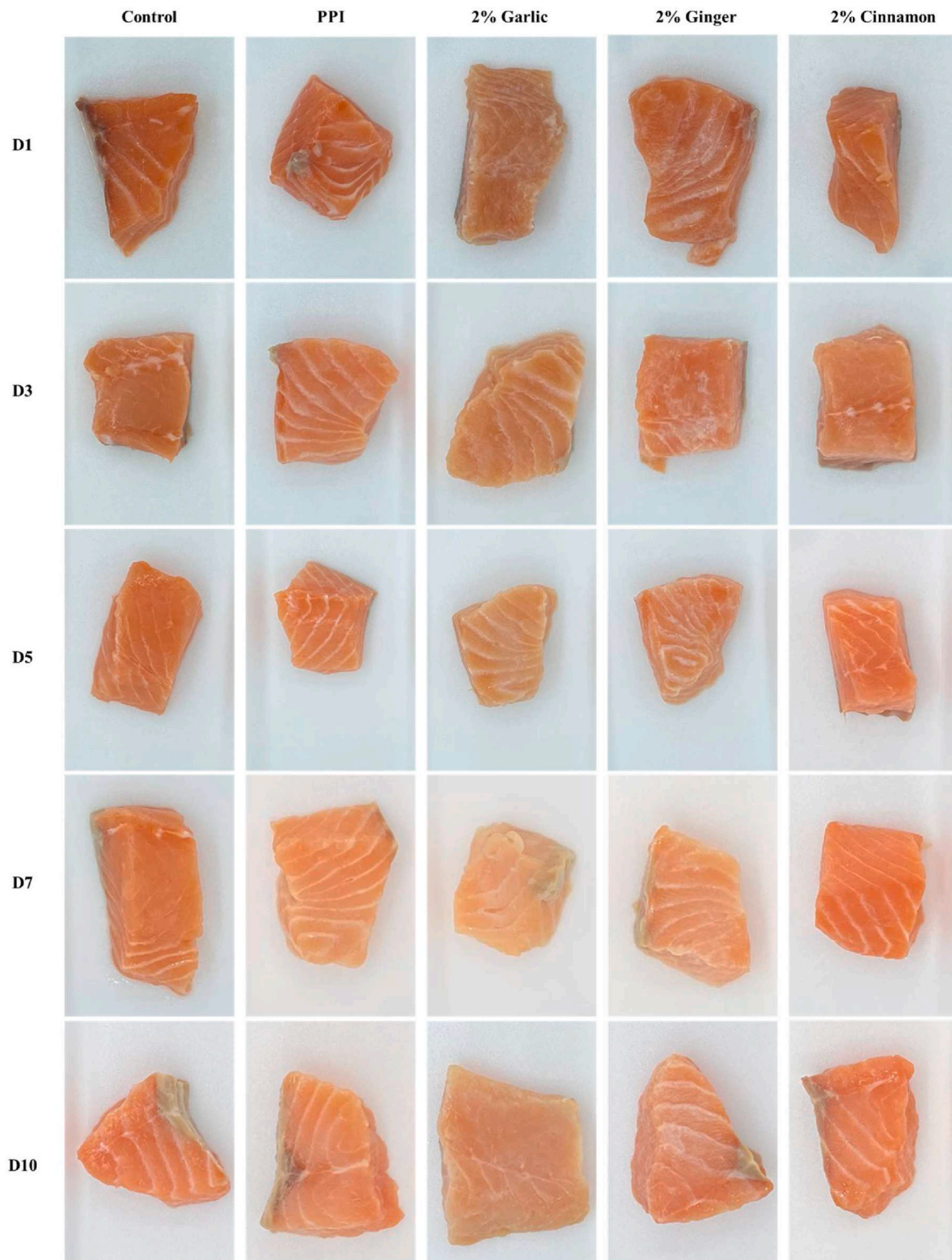


Fig. 6. The appearance of salmon treated with PPI-based active films loaded with garlic, ginger, or cinnamon essential oil at 4 °C over 9 days.

(Estévez and Cava, 2006). Therefore, it is crucial to select the appropriate EO and its concentration for different food systems.

### 3.3.2. Evaluation of antibacterial activity

One aim of incorporating EO into the edible film is to enhance the antibacterial activity of the film, thereby delaying the food spoilage caused by microorganisms. We evaluated the in vitro antibacterial

activity of PPI-based active films against Gram-negative (*S. Typhimurium* and *E. coli*) and Gram-positive bacteria (*S. aureus*), as well as their respective antibacterial effects on salmon. As shown in Table 3, the PPI film did not show antibacterial activity. However, PPI-based films containing 2% garlic, ginger, or cinnamon EOs displayed varying levels of antibacterial activity. Garlic EO was most effective against *S. aureus* but did not affect the growth of *S. Typhimurium* and *E. coli*. In contrast,

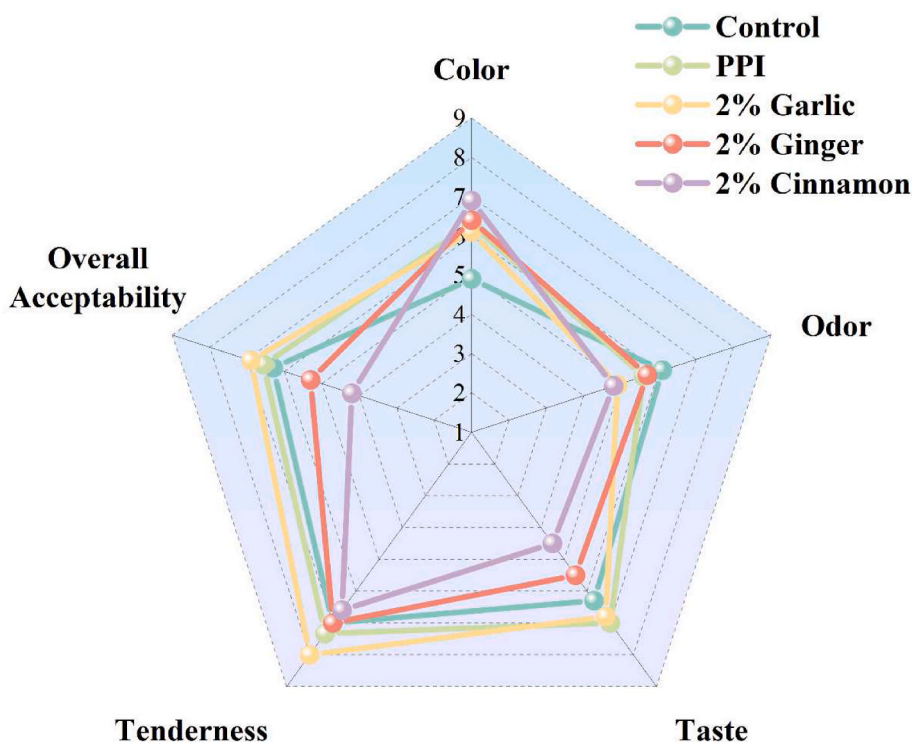


**Fig. 7.** Effects of various PPI film treatments on the sensory attributes (color, odor, taste, tenderness, and overall acceptability) of salmon. (For interpretation of the references to color in this figure legend, the reader is referred to the Web version of this article.)

cinnamon EO showed the strongest antibacterial activity against *S. Typhimurium* and *E. coli* among the three EOs.

Based on the clear inhibition zones shown in Fig. 4, PPI active films with garlic or cinnamon EO were initially expected to effectively inhibit bacterial growth in salmon. However, when applied to salmon, these PPI-based active films showed no significant antibacterial activity (Fig. 5C). On Day 0, the aerobic plate count (APC) of fresh salmon was 2.30 Log CFU/g, and it increased throughout the entire storage period for each group. Moreover, it is noticed that after 9 days of storage at 4 °C, the APC of salmon treated with PPI films containing garlic, ginger, or cinnamon EO did not show notable inhibition compared to the untreated control. These findings indicate that while the active films demonstrated effective antibacterial activity in vitro, this efficacy did not translate to the complex food environment of salmon. The presence of a complex food matrix, along with high fat, protein, and water content in salmon, likely provided ample nutrients for bacteria and bolstered their resilience against the antibacterial agents. The result underscores the critical role of the food system in influencing the performance of active packaging materials.

### 3.3.3. pH, color, and sensory evaluation of salmon during storage

The pH change in fish during storage serves as a reliable indicator of bacterial contamination because spoilage bacteria can produce basic substances like thiocyanate, ammonium, and histamine (Zomorodian et al., 2023). The presence of these compounds increases the pH of fish and reduces its quality. On Day 0, the pH of fresh salmon was 6.18. As depicted in Fig. 5D, salmon treated with various treatments showed no significant difference in pH increase compared to the control group. This observation aligns with the microbiology analysis results (Fig. 5C), where salmon treated with PPI active films did not exhibit inhibited bacterial growth. Consequently, the pH increase trend remained unchanged.

Color is an important quality indicator for salmon, with consumers generally preferring a vibrant red color. Fig. 6 demonstrates that the color of salmon changed after treatment with PPI active films. Initially,

on Day 1, fresh salmon treated with various PPI active films showed no noticeable color change compared to untreated salmon. However, as storage time increased, PPI treatment led to a slight decrease in the redness of salmon. Treatment with PPI loaded with 2% garlic EO resulted in an even paler color of salmon compared to both the control and the PPI treatment, while salmon treated with PPI loaded with 2% cinnamon EO maintained its original color. The red color of salmon comes from carotenoids, especially astaxanthin in the flesh (Skrede and Storebakken, 1986). The fading of redness observed here may be due to interactions between ingredients in the EOs and salmon pigments like carotenoids, causing the salmon to lose its red color. Variations in the color of salmon again highlight the importance of choosing the proper EOs in food packaging to preserve food quality.

In the sensory evaluation, we assessed consumer acceptances for fresh salmon based on color, odor, taste, tenderness, and overall acceptability. The results are shown in Fig. 7. Compared to the control group, coating with PPI films significantly influenced sensory acceptances. The color score increased slightly, while the scores for odor, taste, and tenderness showed varying degrees of decrease across the treatments. PPI film with garlic EO lowered the odor score but improved taste and tenderness. PPI film with ginger EO had no impact on odor or tenderness but reduced the taste score. PPI film with cinnamon EO caused the greatest decrease in odor, taste, and tenderness scores. For overall acceptability, consumers favored untreated salmon, salmon coated with PPI alone, or with PPI and garlic EO over those treated with PPI films containing ginger or cinnamon EO. It is important to note that the scores only reflected consumer acceptance and preference; they do not imply that the original flavor was unaffected by the EOs. In fact, there were notable odor differences between the control and EO-treated groups. Overall, the findings suggest that while PPI films, particularly those with garlic EO, can enhance certain sensory attributes of fresh salmon, the addition of specific EOs, like ginger and cinnamon, may negatively impact consumer acceptance due to changes in odor, taste, and tenderness.

#### 4. Conclusion

This study investigated the impact of incorporating different essential oils (EOs) on the packaging properties of pea protein isolate (PPI) films and their antioxidant and antibacterial activities on salmon. We added 2% garlic, ginger, or cinnamon EO to the PPI film-forming solution and evaluated the resulting films for moisture content (MC), total soluble matter (TSM), water vapor permeability (WVP), water contact angle (WCA), mechanical properties, color, and opacity. Garlic and ginger EOs significantly increased film hydrophobicity, decreasing MC, TSM, and WVP values, while cinnamon EO did not decrease MC and TSM. Cinnamon EO significantly reduced the WCA from 59.01° to 47.52°, whereas garlic and ginger EOs had no effect. Tensile strength (TS) and elongation at break (EAB) decreased with EO addition, with the extent of the decrease ranked as garlic EO < ginger EO < cinnamon EO. SEM images revealed garlic EO was distributed internally, while ginger and cinnamon EOs were on the surface. FTIR analysis confirmed the interactions between PPI and EOs. Peroxide value (PV) and TBARS results for salmon stored at 4 °C for 9 days showed that garlic and ginger EOs in PPI films promoted lipid oxidation, while cinnamon EO significantly prevented it. Despite significant *in vitro* antibacterial activity, these films did not inhibit bacterial growth in salmon. Additionally, EOs in active films could significantly change the color and sensory acceptance of salmon. These findings suggest that the packaging properties of PPI films with EOs depend on the EO type and food system, highlighting the need to select the appropriate EO for specific applications to ensure film efficacy.

#### CRedit authorship contribution statement

**Jingjing Cheng:** Investigation, Formal analysis, Writing – original draft, preparation. **Nethraja Kandula:** Investigation, Formal analysis. **Victoria Eugenia Cortes:** Investigation, Formal analysis. **Hyuk Choi:** Investigation, Formal analysis. **Prashant Singh:** Conceptualization, Formal analysis, Writing – review & editing. **Leqi Cui:** Conceptualization, Supervision, Writing – review & editing.

#### Declaration of competing interest

There are no conflicts to declare.

#### Acknowledgments

This work was supported by the National Institute of Food and Agriculture, US Department of Agriculture (2022-70001-37580).

#### Data availability

Data will be made available on request.

#### References

- Acevedo-Fani, A., Salvia-Trujillo, L., Rojas-Grati, M.A., Martín-Belloso, O., 2015. Edible films from essential-oil-loaded nanoemulsions: physicochemical characterization and antimicrobial properties. *Food Hydrocolloids* 47, 168–177. <https://doi.org/10.1016/j.foodhyd.2015.01.032>.
- Acosta, S., Chiralt, A., Santamarina, P., Rosello, J., González-Martínez, C., Cháfer, M., 2016. Antifungal films based on starch-gelatin blend, containing essential oils. *Food Hydrocolloids* 61, 233–240. <https://doi.org/10.1016/j.foodhyd.2016.05.008>.
- Akhter, R., Masoodi, F.A., Wani, T.A., Rather, S.A., 2019. Functional characterization of biopolymer based composite film: incorporation of natural essential oils and antimicrobial agents. *Int. J. Biol. Macromol.* 137, 1245–1255. <https://doi.org/10.1016/j.ijbiomac.2019.06.214>.
- Al-Harrasi, A., Bhatia, S., Al-Azri, M.S., Ullah, S., Najmi, A., Albratty, M., Meraya, A.M., Mohan, S., Aldawsari, M.F., 2022. Effect of drying temperature on physical, chemical, and antioxidant properties of ginger oil loaded gelatin-sodium alginate edible films. *Membranes* 12. <https://doi.org/10.3390/membranes12090862>.
- Amorati, R., Foti, M.C., Valgimigli, L., 2013. Antioxidant activity of essential oils. *J. Agric. Food Chem.* 61, 10835–10847. <https://doi.org/10.3390/antiox12020383>.

- Aşik, E., Candoğan, K., 2014. Effects of chitosan coatings incorporated with garlic oil on quality characteristics of shrimp. *J. Food Qual.* 37, 237–246. <https://doi.org/10.1111/jfq.12088>.
- ASTM, 1995. *Standard Test Methods for Water Vapor Transmission of Materials 1*.
- Azereido, H.M.C., Otoni, C.G., Mattoso, L.H.C., 2022. Edible films and coatings – not just packaging materials. *Curr. Res. Food Sci.* 5, 1590–1595. <https://doi.org/10.1016/j.crf.2022.09.008>.
- Bahram, S., Rezaei, M., Soltani, M., Kamali, A., Ojagh, S.M., Abdollahi, M., 2014. Whey protein concentrate edible film activated with cinnamon essential oil. *J. Food Process. Preserv.* 38, 1251–1258. <https://doi.org/10.1111/jfpp.12086>.
- Cai, L., Wang, Y., 2021. Physicochemical and antioxidant properties based on fish sarcoplasmic protein/chitosan composite films containing ginger essential oil nanoemulsion. *Food Bioprocess Technol.* 14, 151–163. <https://doi.org/10.1007/s11947-020-02564-0>.
- Cai, L., Wang, Y., Cao, A., 2020. The physicochemical and preservation properties of fish sarcoplasmic protein/chitosan composite films containing ginger essential oil emulsions. *J. Food Process. Eng.* 43, 1–12. <https://doi.org/10.1111/jfpe.13495>.
- Cheng, J., Li, Z., Wang, J., Zhu, Z., Yi, J., Chen, B., Cui, L., 2022. Structural characteristics of pea protein isolate (PPI) modified by high-pressure homogenization and its relation to the packaging properties of PPI edible film. *Food Chem.* 388, 132974. <https://doi.org/10.1016/j.foodchem.2022.132974>.
- Cheng, J., Velez, F.J., Singh, P., Cui, L., 2024. Fabrication, characterization, and application of pea protein-based edible film enhanced by oregano essential oil (OEO) micro- or nano-emulsion. *Curr. Res. Food Sci.* 8, 100705. <https://doi.org/10.1016/j.crf.2024.100705>.
- Cheng, J., Wang, J., Li, Z., Chen, B., Cui, L., 2023. Improving the mechanical and water-resistance properties of pea protein-based edible film via wet-heating Maillard reaction: insights into the simultaneous effect of heating and Maillard reaction. *Food Packag. Shelf Life* 35, 101024.
- Commodity Board, 2024. *Global pea production increase forecasts for fiscal year 2023/24*. Commodity Board [WWW Document].
- Cui, L., Fan, J., Sun, Y., Zhu, Z., Yi, J., 2018. The prooxidant activity of salts on the lipid oxidation of lecithin-stabilized oil-in-water emulsions. *Food Chem.* 252, 28–32. <https://doi.org/10.1016/j.foodchem.2018.01.094>.
- Cui, L., Shen, P., Gao, Z., Yi, J., Chen, B., 2019. New insights into the impact of sodium chloride on the lipid oxidation of oil-in-water emulsions. *J. Agric. Food Chem.* 67, 4321–4327. <https://doi.org/10.1021/acs.jafc.9b00396>.
- Estévez, M., Cava, R., 2006. Effectiveness of rosemary essential oil as an inhibitor of lipid and protein oxidation: contradictory effects in different types of frankfurters. *Meat Sci.* 72, 348–355. <https://doi.org/10.1016/j.meatsci.2005.08.005>.
- Fabra, M.J., Talens, P., Chiralt, A., 2009. Microstructure and optical properties of sodium caseinate films containing oleic acid-beeswax mixtures. *Food Hydrocolloids* 23, 676–683. <https://doi.org/10.1016/j.foodhyd.2008.04.015>.
- Farshi, P., Mirmohammadali, S.N., Rajpurhohit, B., Smith, J.S., Li, Y., 2024. Pea protein and starch: functional properties and applications in edible films. *J. Agric. Food Res.* 15, 100927. <https://doi.org/10.1016/j.jafr.2023.100927>.
- Fathi, N., Almasi, H., Pirouzifard, M.K., 2018. Effect of ultraviolet radiation on morphological and physicochemical properties of sesame protein isolate based edible films. *Food Hydrocolloids* 85, 136–143. <https://doi.org/10.1016/J.FOODHYD.2018.07.018>.
- Fu, L., Xiao, Q., Ru, Y., Hong, Q., Weng, H., Zhang, Y., Chen, J., Xiao, A., 2024. Bio-based active packaging: gallic acid modified agarose coatings in grass carp (*Ctenopharyngodon idellus*) preservation. *Int. J. Biol. Macromol.* 255. <https://doi.org/10.1016/j.ijbiomac.2023.128196>.
- Gao, Q., Feng, Z., Wang, J., Zhao, F., Li, C., Ju, J., 2024a. Application of nano-ZnO in the food preservation industry: antibacterial mechanisms, influencing factors, intelligent packaging, preservation film and safety. *Crit. Rev. Food Sci. Nutr.* 1–27. <https://doi.org/10.1080/10408398.2024.2387327>, 0.
- Gao, Q., Qi, J., Tan, Y., Ju, J., 2024b. Antifungal mechanism of *Angelica sinensis* essential oil against *Penicillium roqueforti* and its application in extending the shelf life of bread. *Int. J. Food Microbiol.* 408.
- Gao, X., Dai, Y., Cao, J., Hou, H., 2023a. Analysis of the effect mechanism of wet grinding on the film properties of pea protein isolate based on its structure changes. *Innovat. Food Sci. Emerg. Technol.* 89. <https://doi.org/10.1016/j.ifset.2023.103474>.
- Gao, X., Dai, Y., Cao, J., Hou, H., 2023b. Analysis of the effect mechanism of wet grinding on the film properties of pea protein isolate based on its structure changes. *Innovat. Food Sci. Emerg. Technol.* 89, 103474. <https://doi.org/10.1016/j.ifset.2023.103474>.
- Ge, J., Sun, C.X., Corke, H., Gul, K., Gan, R.Y., Fang, Y., 2020. The health benefits, functional properties, modifications, and applications of pea (*Pisum sativum* L.) protein: current status, challenges, and perspectives. *Compr. Rev. Food Sci. Food Saf.* 19, 1835–1876. <https://doi.org/10.1111/1541-4337.12573>.
- Ghamari, M.A., Amiri, S., Rezazadeh-Bari, M., Rezazad-Bari, L., 2022. Physical, mechanical, and antimicrobial properties of active edible film based on milk proteins incorporated with *Nigella sativa* essential oil. *Polym. Bull.* 79, 1097–1117. <https://doi.org/10.1007/s00289-021-03550-y>.
- Gomes, A., Costa, A.L.R., Cunha, R.L., 2018. Impact of oil type and WPI/Tween 80 ratio at the oil-water interface: adsorption, interfacial rheology and emulsion features. *Colloids Surf. B Biointerfaces* 164, 272–280. <https://doi.org/10.1016/j.colsurfb.2018.01.032>.
- Grand View Research, 2022. *Salmon fish market size, share & trends analysis report by species (Atlantic/Aquaculture, Pacific), By Form (Fresh, Frozen), By Region, And Segment Forecasts 2022–2030*.
- Haghighatpanah, N., Omar-Aziz, M., Gharaghani, M., Khodaiyan, F., Hosseini, S.S., Kennedy, J.F., 2022. Effect of mung bean protein isolate/pullulan films containing marjoram (*Origanum majorana* L.) essential oil on chemical and microbial properties



- of minced beef meat. *Int. J. Biol. Macromol.* 201, 318–329. <https://doi.org/10.1016/j.ijbiomac.2022.01.023>.
- Hasheminya, S.M., Dehghannya, J., 2021. Development and characterization of novel edible films based on Cordia dichotoma gum incorporated with Salvia mirzayanii essential oil nanoemulsion. *Carbohydr. Polym.* 257, 117606. <https://doi.org/10.1016/j.carbpol.2020.117606>.
- Hematizad, I., Khanjari, A., Basti, A.A., Karabagias, I.K., Noori, N., Ghadami, F., Gholami, F., Teimourifard, R., 2021. In vitro antibacterial activity of gelatin-nanochitosan films incorporated with Zataria multiflora Boiss essential oil and its influence on microbial, chemical, and sensorial properties of chicken breast meat during refrigerated storage. *Food Packag. Shelf Life* 30, 100751. <https://doi.org/10.1016/j.foodpack.2021.100751>.
- Hosseini, M.H., Razavi, S.H., Mousavi, M.A., 2009. Antimicrobial, physical and mechanical properties of chitosan-based films incorporated with thyme, clove and cinnamon essential oils. *J. Food Process. Preserv.* 33, 727–743.
- Kontominas, M.G., Badeka, A.V., Kosma, I.S., Nathanaelides, C.I., 2021. Innovative seafood preservation technologies: recent developments. *Animals* 11, 1–40. <https://doi.org/10.3390/ani11010092>.
- Kowalczyk, D., Gustaw, W., Zieba, E., Lisięcki, S., Stadnik, J., Baraniak, B., 2016. Microstructure and functional properties of sorbitol-plasticized pea protein isolate emulsion films: effect of lipid type and concentration. *Food Hydrocolloids* 60, 353–363. <https://doi.org/10.1016/j.foodhyd.2016.04.006>.
- Kumari, N., Bangar, S.P., Petru, M., Ilyas, R.A., Singh, A., Kumar, P., 2021. Development and characterization of fenugreek protein-based edible film. *Foods* 10. <https://doi.org/10.3390/foods10091976>.
- Lee, D., Tang, J., Lee, S.H., Jun, S., 2024. Effect of oscillating magnetic fields (OMFs) and pulsed electric fields (PEFs) on supercooling preservation of atlantic salmon (*Salmo salar* L.) fillets. *Foods* 13. <https://doi.org/10.3390/foods13162525>.
- Li, C., Pei, J., Xiong, X., Xue, F., 2020. Encapsulation of grapefruit essential oil in emulsion-based edible film prepared by plum (*Pruni domestica* semen) seed protein isolate and gum acacia conjugates. *Coatings* 10. <https://doi.org/10.3390/coatings10080784>.
- Liao, W., Dumas, E., Ghnimi, S., Elaissari, A., Gharsallaoui, A., 2021. Effect of emulsifier and droplet size on the antibacterial properties of emulsions and emulsion-based films containing essential oil compounds. *J. Food Process. Preserv.* 45, 1–10. <https://doi.org/10.1111/jfpp.16072>.
- Liu, M., Pan, Y., Feng, M., Guo, W., Fan, X., Feng, L., Huang, J., Cao, Y., 2022. Garlic essential oil in water nanoemulsion prepared by high-power ultrasound: properties, stability and its antibacterial mechanism against MRSA isolated from pork. *Ultrason. Sonochem.* 90, 106201. <https://doi.org/10.1016/j.ultsonch.2022.106201>.
- McClements, D.J., 2015. *Food Emulsions: Principles, Practices, and Techniques*.
- Moghimi, R., Aliahmadi, A., Rafati, H., 2017. Antibacterial hydroxypropyl methyl cellulose edible films containing nanoemulsions of Thymus daenensis essential oil for food packaging. *Carbohydr. Polym.* 175, 241–248. <https://doi.org/10.1016/j.carbpol.2017.07.086>.
- Muñoz, L.A., Aguilera, J.M., Rodriguez-Turienzo, L., Cobos, A., Diaz, O., 2012. Characterization and microstructure of films made from mucilage of *Salvia hispanica* and whey protein concentrate. *J. Food Eng.* 111, 511–518. <https://doi.org/10.1016/j.jfoodeng.2012.02.031>.
- Noori, S., Zeynali, F., Almasi, H., 2018. Antimicrobial and antioxidant efficiency of nanoemulsion-based edible coating containing ginger (*Zingiber officinale*) essential oil and its effect on safety and quality attributes of chicken breast fillets. *Food Control* 84, 312–320. <https://doi.org/10.1016/j.foodcont.2017.08.015>.
- Pateiro, M., Barba, F.J., Domínguez, R., Sant'Ana, A.S., Mousavi Khaneghah, A., Gavahian, M., Gómez, B., Lorenzo, J.M., 2018. Essential oils as natural additives to prevent oxidation reactions in meat and meat products: a review. *Food Res. Int.* 113, 156–166. <https://doi.org/10.1016/j.foodres.2018.07.014>.
- Pérez Córdoba, L.J., Sobral, P.J.A., 2017. Physical and antioxidant properties of films based on gelatin, gelatin-chitosan or gelatin-sodium caseinate blends loaded with nanoemulsified active compounds. *J. Food Eng.* 213, 47–53. <https://doi.org/10.1016/j.jfoodeng.2017.05.023>.
- Rehman, A., Jafari, S.M., Aadil, R.M., Assadpour, E., Randhawa, M.A., Mahmood, S., 2020. Development of active food packaging via incorporation of biopolymeric nanocarriers containing essential oils. *Trends Food Sci. Technol.* 101, 106–121. <https://doi.org/10.1016/j.tifs.2020.05.001>.
- Santhosh, R., Babu, D.M., Thakur, R., Nath, D., Hoque, M., Gaikwad, K.K., Ahmed, J., Sarkar, P., 2024. Effect of atmospheric cold plasma treatment on structural, thermal, and mechanical properties of pea protein isolate edible films. *Sustain. Chem. Pharm.* 37. <https://doi.org/10.1016/j.scp.2023.101398>.
- Saricaoglu, F.T., Turhan, S., 2020. Physicochemical, antioxidant and antimicrobial properties of mechanically deboned chicken meat protein films enriched with various essential oils. *Food Packag. Shelf Life* 25. <https://doi.org/10.1016/j.foodpack.2020.100527>.
- Skrede, G., Storebakken, T., 1986. Characteristics of color in raw baked and smoked wild and pen-reared atlantic salmon. *J. Food Sci.* 51, 804–808.
- Taha, A., Hu, T., Zhang, Z., Bakry, A.M., Khalifa, I., Pan, S., Hu, H., 2018. Effect of different oils and ultrasound emulsification conditions on the physicochemical properties of emulsions stabilized by soy protein isolate. *Ultrason. Sonochem.* 49, 283–293. <https://doi.org/10.1016/j.ultsonch.2018.08.020>.
- Tan, X., Sun, A., Cui, F., Li, Q., Wang, D., Li, X., Li, J., 2024. The physicochemical properties of Cassava Starch/Carboxymethyl cellulose sodium edible film incorporated of Bacillus and its application in salmon fillet packaging. *Food Chem. X* 23, 101537. <https://doi.org/10.1016/j.fochx.2024.101537>.
- Teixeira, B., Marques, A., Pires, C., Ramos, C., Batista, I., Saraiva, J.A., Nunes, M.L., 2014. Characterization of fish protein films incorporated with essential oils of clove, garlic and organum: physical, antioxidant and antibacterial properties. *Lwt* 59, 533–539. <https://doi.org/10.1016/j.lwt.2014.04.024>.
- Venkatachalam, K., Rakkapao, N., Lekjing, S., 2023. Physicochemical and antimicrobial characterization of chitosan and native glutinous rice starch-based composite edible films: influence of different essential oils incorporation. *Membranes* 13. <https://doi.org/10.3390/membranes13020161>.
- Vidal, N.P., Charlampita, M.C., Spotti, M.J., Martinez, M.M., 2024. Multifunctional phloroglucinol-loaded pea starch coating for refrigerated salmon. *Food Packag. Shelf Life* 43, 101277. <https://doi.org/10.1016/j.foodpack.2024.101277>.
- Vital, A.C.P., Guerrero, A., Ornaghi, M.G., Kempinski, E.M.B.C., Sary, C., Monteschio, J. de O., Matumoto-Pintro, P.T., Ribeiro, R.P., do Prado, I.N., 2018. Quality and sensory acceptability of fish fillet (*Oreochromis niloticus*) with alginate-based coating containing essential oils. *J. Food Sci. Technol.* 55, 4945–4955. <https://doi.org/10.1007/s13197-018-3429-y>.
- Wang, Hang, Wang, Huiyi, Li, D., Luo, Y., 2018. Effect of chitosan and garlic essential oil on microbiological and biochemical changes that affect quality in grass carp (*Ctenopharyngodon idellus*) fillets during storage at 4°C. *J. Aquat. Food Prod. Technol.* 27, 80–90. <https://doi.org/10.1080/10498850.2017.1403525>.
- Wang, W., Zhao, D., Xiang, Q., Li, K., Wang, B., Bai, Y., 2021. Effect of cinnamon essential oil nanoemulsions on microbiological safety and quality properties of chicken breast fillets during refrigerated storage. *LWT—Food Sci. Technol.* 152. <https://doi.org/10.1016/j.lwt.2021.112376>.
- Xu, T., Gao, C.C., Feng, X., Yang, Y., Shen, X., Tang, X., 2019. Structure, physical and antioxidant properties of chitosan-gum Arabic edible films incorporated with cinnamon essential oil. *Int. J. Biol. Macromol.* 134, 230–236. <https://doi.org/10.1016/j.ijbiomac.2019.04.189>.
- Yarnpakdee, S., Benjakul, S., Nalinanon, S., Kristinsson, H.G., 2012. Lipid oxidation and fishy odour development in protein hydrolysate from Nile tilapia (*Oreochromis niloticus*) muscle as affected by freshness and antioxidants. *Food Chem.* 132, 1781–1788. <https://doi.org/10.1016/j.foodchem.2011.11.139>.
- Yu, H., Zhang, C., Xie, Y., Mei, J., Xie, J., 2022. Effect of Melissa officinalis L. essential oil nanoemulsions on structure and properties of carboxymethyl chitosan/locust bean gum composite films. *Membranes* 12. <https://doi.org/10.3390/membranes12060568>.
- Yu, Y.J., Yang, S.P., Lin, T., Qian, Y.F., Xie, J., Hu, C., 2020. Effect of cold chain logistic interruptions on lipid oxidation and volatile organic compounds of salmon (*Salmo salar*) and their correlations with water dynamics. *Front. Nutr.* 7, 1–10. <https://doi.org/10.3389/fnut.2020.00155>.
- Zomorodian, N., Javanshir, S., Shariatifar, N., Rostamnia, S., 2023. The effect of essential oil of Zataria multiflora incorporated chitosan (free form and Pickering emulsion) on microbial, chemical and sensory characteristics in salmon (*Salmo trutta*). *Food Chem. X* 20, 100999. <https://doi.org/10.1016/j.fochx.2023.100999>.
- Zúñiga, R.N., Skurtys, O., Osorio, F., Aguilera, J.M., Pedreschi, F., 2012. Physical properties of emulsion-based hydroxypropyl methylcellulose films: effect of their microstructure. *Carbohydr. Polym.* 90, 1147–1158. <https://doi.org/10.1016/j.carbpol.2012.06.066>.